

Tryptophan Fluorescence Reveals the Presence of Long-Range Interactions in the Denatured State of Ribonuclease Sa

Roy W. Alston,* Mauricio Lasagna,[†] Gerald R. Grimsley,* J. Martin Scholtz,*[†] Gregory D. Reinhart,[†] and C. Nick Pace*[†]

*Department of Molecular and Cellular Medicine, Texas A&M University Health Science Center; and [†]Department of Biochemistry and Biophysics, Texas A&M University, College Station, Texas 77843

ABSTRACT Characterizing the denatured state ensemble is crucial to understanding protein stability and the mechanism of protein folding. The aim of this research was to see if fluorescence could be used to gain new information on the denatured state ensemble. Ribonuclease Sa (RNase Sa) contains no Trp residues. We made five variants of RNase Sa by adding Trp residues at locations where they are found in other members of the microbial ribonuclease family. To better understand the protein denatured state, we also studied the fluorescence properties of the following peptides: *N*-acetyl-Trp-amide (NATA), *N*-acetyl-Ala-Trp-Ala-amide (AWA), *N*-acetyl-Ala-Ala-Trp-Ala-Ala-amide (AAWAA), and the five pentapeptides with the same sequence as the Trp substitution sites in RNase Sa. The major conclusions are: 1), the wavelength of maximum fluorescence intensity, λ_{\max} , does not differ significantly for the peptides and the denatured proteins; 2), the fluorescence intensity at λ_{\max} , I_F , differs significantly for the five Trp containing variants of RNase Sa; 3), the I_F differences for the denatured proteins are mirrored in the peptides, showing that the short-range effects giving rise to the I_F differences in the peptides are also present in the proteins; 4) the I_F values for the denatured proteins are more than 30% greater than for the peptides, showing the presence of long-range effects in the proteins; 5), fluorescence quenching of Trp by acrylamide and iodide is more than 50% greater in the peptides than in the denatured proteins, showing that long-range effects limit the accessibility of the quenchers to the Trp side chains in the proteins; and 6), these results show that nonlocal effects in the denatured states of proteins influence Trp fluorescence and accessibility significantly.

INTRODUCTION

There is considerable interest in gaining a better understanding of the denatured states of proteins. This has become more important now that we know some proteins are unfolded under physiological conditions (1,2). Both protein stability (3–5) and the mechanism of protein folding (6–8) depend on the properties and concentrations of the molecules that make up the denatured state ensemble of a protein. The primary goal of this research was to see if the fluorescence properties of the tryptophan residues in a protein could be used to gain a better understanding of the denatured state ensemble. This was investigated with different approaches in several early studies (9–11) and in many recent studies (12–24).

Our broad view of the structure of globular proteins has not changed since the first high resolution crystal structures became available in the early 1960s, but our detailed view of the structure of the native state ensemble of proteins has increased greatly (25). In contrast, our understanding of the denatured state has changed over the years and is still in a state of flux (26–28). Tanford et al. carried out the first careful studies of the denatured states of proteins and concluded that proteins approach a randomly-coiled conformation in 6 M GdnHCl and 8 M urea with their disulfide bonds broken (29). It was clear to

Tanford that pockets of structure might exist, and this was emphasized at the time by polymer chemists (30). More recent studies of the denatured state using small angle x-ray scattering to determine the radius of gyration, or pulsed-field-gradient NMR to estimate the hydrodynamic radius have reached similar conclusions (31). Observations by Shortle et al. began to change the way we envision the denatured states of proteins. They confirmed the idea that pockets of structure exist and that the denatured state is more compact than the hydrodynamic studies led many of us to believe (32).

Proteins are unfolded to a great extent in urea and GdnHCl solutions, but hydrophobic clusters, α -helices, β -sheets, and other native-like structures can exist even under strongly denaturing conditions (28,33–37). NMR is beginning to give a clearer picture of the denatured state ensemble that exists under physiological conditions, the denatured state of most interest to us (36,38–40). Choy et al. (41) have shown that the molecules in the denatured state ensemble are relatively compact, ~30–40% larger than the native state. Mayor et al. (42) studied the denatured state of the engrailed homeodomain and concluded: “The denatured state had extensive native secondary structure and was significantly compact and globular. But, the side-chains and backbone were highly mobile.”

Computational studies have improved our understanding of the denatured state ensemble of proteins (43–47). Just taking excluded volume into account suggests a compact denatured state in which the radius of gyration is closer to that expected for a native protein, but the solvent accessibility is closer to that expected for an extended chain (43). More

Submitted July 6, 2007, and accepted for publication November 7, 2007.

Address reprint requests to C. Nick Pace, Tel.: 979-845-1788; Fax: 979-847-9481; E-mail: nickpace@tamu.edu.

Roy W. Alston's present address is Biogen Idec, Protein Formulation and Development, 5200 Research Place, San Diego, CA 92112.

Editor: Kathleen B. Hall.

recent studies are taking into account additional important effects that should lead to better insight into the denatured state ensemble of proteins (45,46).

Ribonuclease Sa (RNase Sa) is a small (96 amino acids) globular protein in the microbial ribonuclease family. Over the past 20 years, our laboratory has used RNase Sa as a model to gain a better understanding of protein structure and stability (see (48–50) and earlier studies). The crystal structure of the protein has been determined at 1.0 Å resolution by Sevcik et al. (51) and a solution structure has been determined using NMR by Laurents et al. (52). In addition, the pK values of the ionizable groups in the native state were measured recently (53,54), and studies of the pKs in the denatured state are almost completed.

RNase Sa contains no tryptophan residues. In a previous study, we inserted tryptophans at four locations where tryptophans are found in other microbial ribonucleases, and studied the fluorescence properties and stabilities of these variants (55). The emphasis of that study was on the fluorescence properties of the native state of the proteins, but some studies were done on the denatured states in 9 M urea. The results showed clearly that the fluorescence properties of the denatured proteins differed. This study is a continuation of that work. We report studies of five single Trp variants of RNase Sa: D1W, Y52W, Y55W, T76W, and Y81W. These proteins were studied in concentrated urea and GdnHCl solutions with their disulfide bonds broken. The results show that long-range effects in a denatured protein can significantly effect the fluorescence properties.

MATERIALS AND METHODS

Materials

3-[*N*-morpholino] propane sulfonic acid (MOPS) were obtained from Sigma-Aldrich (St. Louis, MO). Ultra-pure urea was obtained from Nacalai Tesque (Kyoto, Japan), and ultra-pure GdnHCl was obtained from ICN Biomedicals (Aurora, OH). Urea and GdnHCl stock solutions were prepared by weight, and the concentrations were determined as described previously (56). All other reagents were of analytical grade. Wild-type and variant forms of RNase Sa were prepared and purified as described previously (55,57,58).

Preparation of protein solutions

The single disulfide bond in the RNase Sa variants was reduced with 10 mM Tris (2-carboxyethyl) phosphine HCl (TCEP) for all of the experiments described in this study. Protein concentrations of RNase Sa solutions were determined spectrophotometrically using a Gilford Model 250 spectrophotometer. The molar absorption coefficient of $\epsilon_{280} = 12,045 \text{ M}^{-1} \text{ cm}^{-1}$ was used for wild-type RNase Sa (57). For the tyrosine to tryptophan variants, a molar absorption coefficient of $\epsilon_{280} = 16,055 \text{ M}^{-1} \text{ cm}^{-1}$ was used. For D1W and T76W $\epsilon_{280} = 17,545 \text{ M}^{-1} \text{ cm}^{-1}$ was used. These are based on the average molar absorption coefficients observed for Tyr and Trp residues in proteins (59). The error in determining the protein concentration using these predicted extinction coefficients is <3%.

Fluorescence emission spectra

Protein samples with 10 μM concentrations in 30 mM MOPS buffer, pH 7.0, 25°C were studied in two denaturing solutions: 8.5 M urea and 6 M GdnHCl.

For all of the protein measurements, the disulfide bond in the proteins was reduced with 10 mM TCEP. All fluorescence emission spectra were determined and analyzed as described in the companion study (60).

As with the peptides (60), we determined ϵ_{300} and $\epsilon_{298-302}$ values for three of the proteins, D1W, T76W, and Y55W, again, in units of $\text{M}^{-1} \text{ cm}^{-1}$. We found: $\epsilon_{300} = 1069$ (D1W), 1011 (T76W), and 1119 (Y55W); and the $\epsilon_{298-302} = 1107$ (D1W), 1046 (T76W), and 1155 (Y55W). The average values are $\epsilon_{300} = 1066 \pm 54$ and $\epsilon_{298-302} = 1103 \pm 55$. These values do not differ significantly and we conclude that the absorption spectra are not shifted significantly. The average values for the proteins are higher than the average values for the peptides. As with the peptides, we think this results because the proteins contain either 7 or 8 Tyr residues and they do make a small contribution to the light absorption at 300 nm. For the four small molecules with a single Trp and no Tyr residues (60), the average $\epsilon_{300} = 956 \pm 30$. Based on our results, we estimate that the Trp contribute ~ 950 and the Tyr 50 ± 30 to the ϵ_{300} and $\epsilon_{298-302}$ values. However, there should be minimal energy transfer from the Tyr to the Trp residues in unfolded protein so the light absorbed by the Tyr should make only a small contribution to the fluorescence of the Trp residues. In conclusion, the small differences in light absorption among the peptides and proteins should make only a small contribution to our results and cannot account for the 30% larger I_F values observed for the proteins compared with the peptides.

Acrylamide and iodide quenching

The quenching experiments were done on the protein solutions at a concentration of 10 μM at pH 7.0, 25°C in 30 mM MOPS buffer in the presence of 7.6 M urea or 3.8 M GdnHCl and 10 mM TCEP. It was necessary to use lower concentrations of urea and GdnHCl than those used for the fluorescence emission experiments because iodide was not soluble at higher urea and GdnHCl concentration. However, the denaturant concentrations used were well above those needed to completely unfold the proteins (61). The measurements were made and the data analyzed as described in the companion study (60). Each experiment was carried out at least twice and the results were averaged. The results always differed by <1.7%, and generally by <1%.

Time-resolved fluorescence measurements

Time-resolved fluorescence experiments were carried out as described in the companion study (60).

RESULTS

The proteins studied in this research were the following single-site Trp variants of RNase Sa: D1W, Y52W, Y55W, T76W, and Y81W. The location of these Trp residues in RNase Sa is shown in Fig. 1. To gain a better understanding of the results obtained with these proteins, six pentapeptides were also studied: AAWAA, WVSGT (D1W), GYWHE (Y52W), HEWTV (Y55W), EAWQE (T75W), and DYWTG (Y81W). The latter five peptides have the same sequence as those surrounding the tryptophans in the proteins. For WVSGT, the peptide model for D1W, the amino terminal amino group was not acetylated. For all of the other peptides, the α -amino group was acetylated and the α -carboxyl group was amidated. The results with the peptides were described in the companion study (60), but some of the results are also given in this study. The parameters measured were the spectral moment, SM, the wavelength where the fluorescence

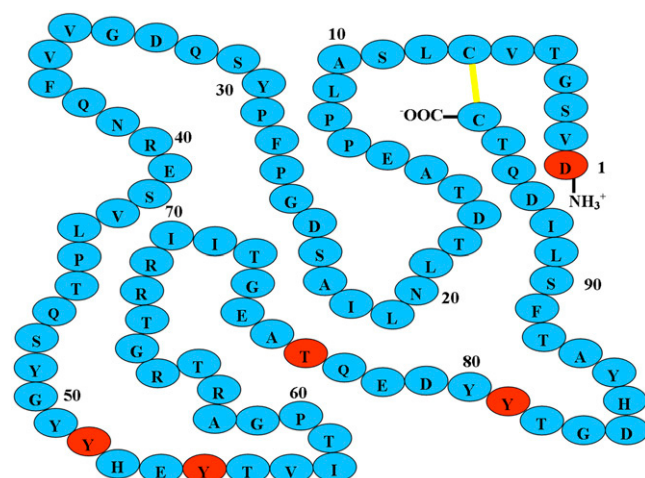


FIGURE 1 Amino acid sequence of RNase Sa showing the positions, colored red, where Trp residues were added for the studies described in this study. The yellow line shows the position of the disulfide bond present in native RNase Sa. This disulfide bond was reduced and the proteins unfolded for all of the studies reported here.

intensity is maximal, λ_{\max} , the fluorescence intensity at λ_{\max} , I_F , the Stern-Volmer quenching constant, K_{SV} , the average excited state lifetime, τ_{ave} , and the width of the lifetime distribution. The SM is included in the table, but will not be discussed in this study.

Fluorescence emission spectra

Typical fluorescence emission spectra for the reduced, denatured proteins are shown in Fig. 2. The parameters characterizing these spectra in 8.5 M urea and in 6 M GdnHCl are given in Table 1. The λ_{\max} values for the pentapeptides and proteins do not differ significantly. As with the peptides, the I_F values are always greater in urea than they are in GdnHCl (3–24%

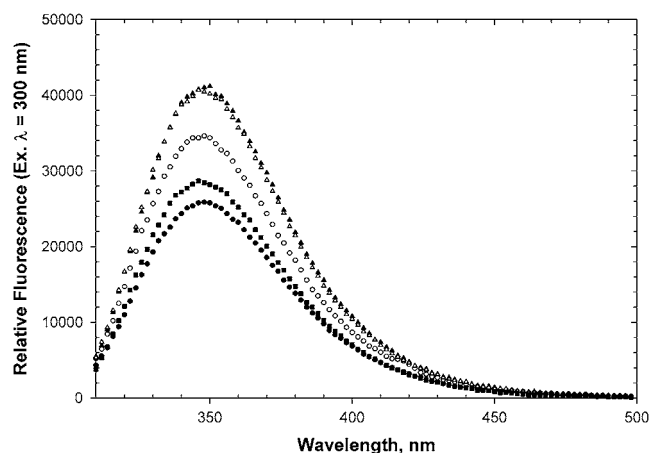


FIGURE 2 Fluorescence emission spectra after 300 nm excitation for five denatured, reduced RNase Sa Trp variants at 10 μ M concentration in 8.5 M urea, 10 mM TCEP, pH 7.0, and 25°C. D1W (●), Y52W (○), Y55W (▲), T76W (△), and Y61W (■).

greater). The most interesting finding is that the I_F values of the proteins differ significantly and that they are all substantially higher than the values for the corresponding peptides.

Fluorescence quenching by acrylamide and iodide

Typical Stern-Volmer plots for the quenching of the Trp fluorescence of the reduced, denatured RNase Sa variants by iodide in 3.8 M GdnHCl are shown in Fig. 3. The Stern-Volmer quenching constants characterizing the results in urea and GdnHCl are given in Table 2. In urea solutions, the K_{SV} values for acrylamide quenching are always significantly greater than the values for iodide quenching, but this is not true in the GdnHCl solutions. The K_{SV} value for the amino terminal Trp residues is always substantially greater than the K_{SV} values for the Trp at internal residues. The most interesting finding is that the K_{SV} values of the proteins differ and that they differ from the values obtained for the peptides.

Fluorescence excited-state lifetimes

Time-resolved fluorescence measurements were carried out as described above. The results for the reduced, denatured proteins are given in Table 3. For all of the variants except D1W, the fluorescence excited-state lifetimes showed a Gaussian distribution and the τ_{ave} value and the width of the distribution are given in Table 3. The τ_{ave} value is the center of the Gaussian distribution. For D1W, the results were fit to a Gaussian distribution plus a discrete component.

DISCUSSION

Five Trp variants of RNase Sa

Fig. 1 shows the positions of the Trp residues in the RNase Sa variants studied here. The figure also shows the location of the disulfide bond, but for all of the studies reported here, the disulfide bond is reduced and the proteins are unfolded. For D1W, there is a positive charge on the α -amino group of the N-terminal Trp. For Y55W, the Glu adjacent to the Trp will have a negative charge, and for Y52W the His adjacent to the Trp will have a positive charge of ~ 0.5 (54). If we use the size of the adjacent side chains as a measure of solvent accessibility, the Trp accessibility will decrease in this order: D1W > T76W > Y55W > Y81W > Y52W. Tables 4 and 5 compare the results for the RNase Sa variants with the results for the pentapeptides from the companion study (60).

Fluorescence emission spectra

λ_{\max} values for the peptides and proteins do not differ significantly

The observed λ_{\max} values for Trp residues in proteins range from 308 to 355 nm (62,63). In general, the more buried the

TABLE 1 Comparison of the fluorescence properties of the reduced, denatured tryptophan variants of RNase Sa in 8.5 M urea and 6 M guanidine hydrochloride, pH 7.0, and 25°C

Variant	SM* (nm)	SM (nm)	λ_{\max}^{\dagger} (nm)	λ_{\max} (nm)	I_F at λ_{\max}^{\dagger}	I_F at λ_{\max}	% Δ^{\S}
	Urea	GdnHCl	Urea	GdnHCl	Urea	GdnHCl	
D1W	361	363	345	351	25,900	25,000	3
Y52W	360	360	348	347	34,600	30,700	11
Y55W	360	361	350	346	41,200	33,800	18
T76W	360	361	346	346	40,700	31,100	24
Y81W	359	360	347	346	28,700	26,000	9

*Spectral moment (SM) is the wavelength at which the total area under the emission spectrum is divided into two equal areas.

λ_{\max}^{\dagger} is the wavelength of maximum fluorescence intensity. We estimate the error to be ± 2 nm.

I_F at λ_{\max} is the fluorescence intensity at λ_{\max} . We estimate the error to be $\pm 3\%$.

$\% \Delta = ((I_{F,Urea} - I_{F,GdnHCl})/I_{F,Urea}) \times 100$.

Trp residue in the protein, the greater the blue shift of λ_{\max} (64). Tew and Bottomley (17) studied two Trp residues in α_1 -antitrypsin and showed that in 8 M urea $\lambda_{\max} = 353$ nm for Trp 194, but $\lambda_{\max} = 345$ nm for Trp238. They concluded: "In the urea-induced unfolded state, Trp238 does not become fully solvated, suggesting the persistence of structure around the residue." This encouraged us to see whether λ_{\max} might detect structure surrounding the Trp side chains in the denatured state ensembles of our RNase Sa variants.

In an earlier study (55), we showed that the λ_{\max} values are blue-shifted to shorter wavelengths in the folded proteins: 309 nm (Y52W), 310 nm (Y55W), 335 nm (T76W), and 319 nm (Y81W). In folded RNase Sa, these blue shifts correlate with the % burial of the side chains they replace: Y52 98%, Y55 91%, T764%, and Y81 87%. For the five Trp variants in unfolded RNase Sa, the λ_{\max} values in urea range from 345 to 350 with an average of 347.2 ± 1.9 nm and the values in GdnHCl range from 346 to 351 nm with an average of 347.2 ± 2.2 nm (Tables 4 and 5). For the five pentapeptides, the λ_{\max} values in urea range from 347 to 349 nm with an average of

347.4 ± 0.9 nm, and those in GdnHCl range from 347 to 350 nm with an average of 348.2 ± 1.3 nm (Tables 4 and 5). The maximum difference between the λ_{\max} value for a protein and its corresponding pentapeptide is 3 nm. Thus, the λ_{\max} values for the pentapeptides do not differ significantly from those for the unfolded proteins, and provide no evidence for structure in the denatured ensemble that would bury the indole group enough to shift the λ_{\max} value to lower wavelengths. The results with α_1 -antitrypsin show that this will not always be the case (17). The denatured state ensemble in equilibrium with the folded protein under physiological conditions is generally thought to be more compact than in the presence of strong denaturants like urea and GdnHCl (18,37). Consequently, there will be a better chance of observing shifts in λ_{\max} when the denatured state that exists under physiological conditions is studied. For example, shifts in λ_{\max} have been observed for Trp residues in the molten globulin state of α -lactalbumin (65), and in folding intermediates of Barstar (20). As we will discuss next, the λ_{\max} values are less sensitive to structure in the denatured state ensembles than the I_F values.

Factors contributing to I_F

As described in the companion study (60), experimental (66–69) and theoretical (68,70,71) results suggest that electron transfer from Trp to the carbonyl group of peptide bonds is

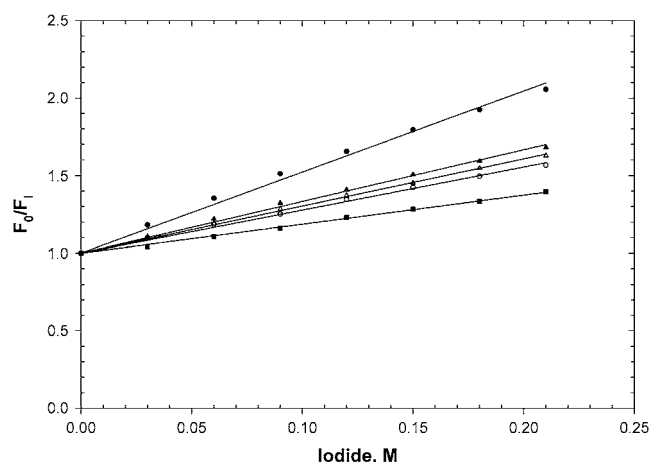


FIGURE 3 Iodide fluorescence quenching (300 nm excitation, 350 nm emission) of five denatured, reduced RNase Sa Trp variants at 10 μ M concentration in 7.6 M urea, 10 mM TCEP, pH 7.0, and 25°C. D1W (●), Y52W (○), Y55W (▲), T76W (Δ), and Y58W (■).

TABLE 2 Stern-Volmer constants for acrylamide and iodide quenching of the fluorescence of the reduced, denatured tryptophan variants of RNase Sa in 7.6 M urea and 3.8 M guanidine hydrochloride, pH 7.0, and 25°C*

Variant	Acrylamide K_{SV} (M^{-1})		Iodide K_{SV} (M^{-1})	
	Urea	GdnHCl	Urea	GdnHCl
D1W	10.04	8.38	5.23	4.59
Y52W	7.20	6.87	2.77	3.06
Y55W	8.52	7.97	3.33	3.22
T76W	7.92	7.57	3.04	2.92
Y81W	6.15	5.96	1.87	2.47

*Calculated as described in Materials and Methods. We estimate the error for K_{SV} to be $\leq 3\%$.

TABLE 3 Average fluorescence lifetimes determined by analyzing a Gaussian distribution of the lifetimes for the reduced, denatured tryptophan variants of RNase Sa in 8.5 M urea and 6 M guanidine hydrochloride, pH 7.0, and 25°C

Variant	τ_{ave}^* (ns)	τ_{ave}^* (ns)	Width (ns)		χ^2	χ^2
	Urea	GdnHCl	Urea	GdnHCl	Urea	GdnHCl
D1W	4.79 \pm 0.06	3.89 \pm 0.07	3.09 \pm 0.03	2.57 \pm 0.08	0.79	1.95
Y52W	3.46 \pm 0.10	2.85 \pm 0.05	1.70 \pm 0.11	1.30 \pm 0.06	1.99	1.28
Y55W	4.02 \pm 0.09	3.17 \pm 0.04	1.72 \pm 0.08	1.30 \pm 0.04	1.46	1.55
Y76W	3.94 \pm 0.08	2.93 \pm 0.04	1.62 \pm 0.08	1.12 \pm 0.03	1.52	1.02
Y81W	3.24 \pm 0.09	2.70 \pm 0.07	1.63 \pm 0.08	1.24 \pm 0.08	1.43	1.98

* τ -value at the center of the Gaussian distribution.

the most important mechanism for intramolecular quenching of Trp fluorescence. The pentapeptides have six backbone carbonyls per molecule, but the RNase variants have 95. This suggested to us that the proteins would have lower fluorescence intensities than the pentapeptides, but this is not observed. Engelborgh et al. (68) analyzed the electron transfer process from the indole C ϵ 3 atom to the carbonyl carbon of the nearest peptide bond for the Trp residues in several different folded proteins. They showed that the rate constant for electron transfer at the van der Waals contact distance (3 Å) was 5.0 (ns)⁻¹ and decreased to zero beyond \sim 5 Å. Thus, electron transfer will be important only at short distances (3–5 Å) and this makes the conformation of the Trp and neighboring carbonyl groups very important.

As with the peptides, there is an excellent correlation between the I_F values and the τ_{ave} values, except for the protein and peptide with the Trp residue at the amino terminus. When these two values are excluded, the correlation coefficient is 0.94 for the four protein values and the 7 peptide values for the data in urea. This is discussed in the companion study.

Short-range quenching in proteins mimics that observed in peptides

The I_F values for the proteins correlate well with the values for the corresponding pentapeptides. If we just consider the Trp residues at internal positions, the correlation coefficient

is 0.97 for the I_F values in both urea and GdnHCl. This shows that the short-range effects that cause the differences between the I_F values for the individual peptides also contribute to the differences observed for the proteins. Studies by Barkley and Pan have shown that the ϕ -, ψ -angles, and the χ_1 rotamer populations of Trp residues in cyclic hexapeptides vary with position in the sequence and influence the quantum yield (69). Similarly, the differences in amino acid sequence in the pentapeptides studied here will influence their conformational ensembles and this is probably the most important factor that determines the differences in the I_F values (60). The short-range effects observed in the peptides seem to exert a similar influence in the proteins.

Protein I_F values are over 30% higher than those for peptides

Surprisingly, the proteins always have substantially larger I_F values than the corresponding peptides. For the four variants with Trp at internal positions, the protein I_F values in urea are 10,000 (W52), 10,400 (W55), 8,400 (W76), and 7,200 (W81) higher than for the peptides (Table 4). Similar large differences are observed in GdnHCl. The protein I_F values average 34% higher than the peptides in urea and 33% higher in GdnHCl. Thus, there is a long-range effect observed only in the proteins that is superimposed on the short-range effects seen in both the peptides and the proteins. If we interpret this in terms of carbonyl group quenching, it suggests that the

TABLE 4 Fluorescence properties of the peptides and the reduced, denatured tryptophan variants of RNase Sa in urea, pH 7.0, and 25°C

Peptide/variant	λ_{max}^* (nm)	I_F at $\lambda_{\text{max}}^{\dagger}$ (nm)	$\tau_{\text{ave}}^{\ddagger}$ (ns)	k_q^{\S} (M ⁻¹ ns ⁻¹)	
				Acrylamide	Iodide
NATA	352	49,000	4.04	4.92	2.19
AWA	349	24,400	2.44	4.00	1.61
AAWAA	350	28,500	2.80	3.52	1.44
WVSGT/D1W	347/345	23,900/25,900	4.59/4.79	2.79/2.10	1.68/1.09
GYWHE/Y52W	347/348	24,600/34,600	2.25/3.46	3.51/2.08	1.17/0.80
HEWTV/Y55W	349/350	30,800/41,200	2.95/4.02	3.41/2.12	1.26/0.83
EAWQE/T76W	347/346	32,300/40,700	3.10/3.94	3.09/2.01	0.94/0.77
DYWTG/Y81W	347/347	21,500/28,700	2.48/3.24	3.38/1.90	1.00/0.58

*From Table 1 of the companion study (60) and Table 1 of this work.

\dagger From Table 1 of the companion study (60) and Table 1 of this work.

\ddagger From Table 3 of the companion study (60) and Table 3 of this work.

$\S k_q = K_{SV}/\tau_{\text{ave}}$ where the K_{SV} values are taken from Table 2 of the companion study (60) and Table 2 of this work.

TABLE 5 Fluorescence properties of the peptides and the reduced, denatured tryptophan variants of RNase Sa in guanidine hydrochloride, pH 7.0, and 25°C

Peptide/variant	λ_{max}^* (nm)	I_F at $\Delta_{\text{max}}^\dagger$ (nm)	$\tau_{\text{ave}}^\ddagger$ (ns)	$k_q^§$ ($\text{M}^{-1} \text{ns}^{-1}$)	
				Acrylamide	Iodide
NATA	351	35,500	2.80	6.03	2.43
AWA	346	22,100	1.90	5.17	1.80
AAWAA	350	23,100	2.05	4.22	1.56
WVSGT/D1W	350/351	22,100/25,000	3.80/3.89	2.77/2.15	1.41/1.18
GYWHE/Y52W	347/347	23,100/30,700	2.01/2.85	3.78/2.41	1.42/1.07
HEWTV/Y55W	349/346	25,700/33,800	2.42/3.17	3.66/2.51	1.40/1.02
EAWE/T76W	348/346	24,900/31,100	2.30/2.93	3.51/2.58	1.33/1.00
DYWTG/Y81W	347/346	18,400/26,000	3.80/3.89	3.77/2.21	1.24/0.91

*From Table 1 of the companion study (60) and Table 1 of this work.

†From Table 1 of the companion study (60) and Table 1 of this work.

‡From Table 3 of the companion study (60) and Table 3 of this work.

§ $k_q = K_{SV}/\tau_{\text{ave}}$ where the K_{SV} values are taken from Table 2 of the companion study (60) and Table 2 of this work.

carbonyl groups in the peptides are closer to the Trp side chains than those in the proteins. This longer range effect may depend, in part, on the flexibility of the polypeptide chain near the Trp. Eftink et al. (67) noted: “The fluorescence quantum yields of the constrained analogs are higher than those for the unconstrained counterparts.” Perhaps, the Trp quenching by the carbonyl groups of the peptide bonds becomes less efficient as the polypeptide chain becomes longer because they become less flexible. Recall, that the four carbonyls in AWA were better able to quench the fluorescence than the six carbonyls in AAWAA. The flexibility possible in the shorter peptides may allow more conformations in which the Trp fluorescence can be quenched by the neighboring carbonyls than in the proteins. This idea is supported by the I_F values observed for the peptide and protein with the amino terminal Trp. Here, the I_F values differ much less than when the Trp is at an internal position (Tables 4 and 5). Even though protein denatured states are known to be quite compact (72) and contain appreciable secondary structure (28), only the neighboring carbonyl groups seem to contribute significantly to Trp quenching. This might not be the case if a hydrophobic pocket were present containing a Trp residue, as has been observed in some cases (21,36,73).

Studies of model compounds have shown that Trp quenching by carbonyls is extremely sensitive to structure and conformation, and that it only occurs in polar solvents (66,67,69). This suggests another possibility for the long-range effect observed with the proteins. Perhaps the compact denatured states of proteins provide a more nonpolar environment that diminishes the quenching due to electron transfer from Trp to the neighboring carbonyls. This idea is supported by the results discussed next that show that acrylamide and iodide quenching are both much less efficient in proteins than in peptides.

On average, the differences between the I_F values in urea and GdnHCl solutions are greater for the proteins than for the peptides. We have shown previously that electrostatic interactions in the denatured state ensemble of RNase Sa can

affect both the energetics (3), and kinetics (6) of folding. Others have made similar observations in other proteins (4,5,7,8). Thus, it is not surprising that a change in solvent that is accompanied by a large change in dielectric constant could influence the denatured state ensemble of a protein more than the conformational ensemble of a pentapeptide.

Fluorescence quenching by acrylamide and iodide

Quenching is reduced significantly in proteins compared with peptides

The k_q values should depend mainly on the accessibility of the Trp side chains to the quencher. Qualitatively, the results support this idea. For the peptides, k_q values decrease in the order NATA > AWA > pentapeptides with internal Trp for both acrylamide and iodide quenching (Tables 4 and 5). This becomes even more evident when we consider the results for the proteins, where k_q values are always substantially less than values for the peptides. For the Trp residues at internal positions, the differences are quite striking. For acrylamide quenching, the peptide k_q values average 66% larger than the protein values in urea and 53% larger in GdnHCl. For iodide quenching, the values average 48% larger in urea and 35% larger in GdnHCl. This shows that Trp residues in unfolded proteins are much less accessible to a quencher than in pentapeptides with the same sequence.

For the proteins, k_q values for acrylamide quenching observed when the Trp residues are at internal positions range from 1.90 to 2.12 $\text{M}^{-1} \text{ns}^{-1}$ in urea and from 2.21 to 2.58 $\text{M}^{-1} \text{ns}^{-1}$ in GdnHCl, and the values for the N-terminal Trps are 2.10 $\text{M}^{-1} \text{ns}^{-1}$ in urea and 2.15 $\text{M}^{-1} \text{ns}^{-1}$ in GdnHCl (Tables 4 and 5). (If the discrete component is taken into account, the k_q values for the N-terminal Trps are increased to 2.35 $\text{M}^{-1} \text{ns}^{-1}$.) The range in values is small, and the N-terminal Trp residue seems, unexpectedly, to be comparable in accessibility to those at internal positions. This was also

observed with the peptides and again suggests that quenching of the N-terminal Trp by acrylamide is less than expected based on its exposure. The reasons for this are not clear.

For the proteins, k_q values for iodide quenching observed when the Trp residues are at internal positions range from 0.58 to 0.80 $\text{M}^{-1} \text{ns}^{-1}$ in urea and from 0.91 to 1.07 $\text{M}^{-1} \text{ns}^{-1}$ in GdnHCl, and the values for the N-terminal Trps are 1.09 $\text{M}^{-1} \text{ns}^{-1}$ in urea and 1.18 $\text{M}^{-1} \text{ns}^{-1}$ in GdnHCl (Tables 4 and 5). (If the discrete component is taken into account, the k_q values for the N-terminal Trps are increased to 1.22 $\text{M}^{-1} \text{ns}^{-1}$ in urea and 1.30 $\text{M}^{-1} \text{ns}^{-1}$ in GdnHCl.) As with acrylamide, the range is still small, but now the k_q values are greater for the N-terminal Trps, as expected. This probably reflects the greater accessibility of the side chain of the N-terminal Trp residue, and the favorable charge–charge interactions between the iodide ion and the positive charge on the α -amino group.

For NATA and all of the peptides and proteins, k_q values are always smaller in urea solutions than in GdnHCl solutions, but the correlation coefficient between the k_q values is 0.97 for acrylamide and 0.94 for iodide. This suggests that the effect is general and does not depend on the specific sequence. As discussed in the companion study (60), this probably results simply because the relative viscosity of the 3.8 M GdnHCl solutions is 1.25 and the relative viscosity of the 7.6 M urea solutions is 1.60. The viscosity dependence of the quenching of peptides and proteins was previously studied by Eftink and Hagaman (74).

Relationship between I_F and k_q

If we compare the I_F values with the k_q values for acrylamide quenching, the values are always lowest for Y81W and highest for Y55W. The lower k_q values suggest that the Trp 81 is less exposed to quencher so the denatured state is more compact. This would also be expected to lead to a lower I_F value for the reasons discussed above. The opposite would be expected for Y55W. This seems to be a long-range effect. If it were a short-range effect based on accessibility, we would expect Y52W to have the lowest k_q value and T76W to have the greatest. The results from iodide quenching are more complicated, probably because of the contribution of charge–charge interactions.

CONCLUDING REMARKS

As discussed in the companion study, adjacent side chains that are known to quench Trp fluorescence do not seem to make a large contribution to the differences among the I_F values for the peptides. We suggested that differences in the I_F values of the individual peptides depended more on the effect of sequence on local conformations than on side chain quenching. The good correlation between the I_F values of the proteins and the corresponding peptides suggests that this is also true in the proteins. However, the I_F values for the proteins are always substantially higher than those of the

peptides. There is a long-range effect observed only in the proteins that is superimposed on the short-range effect observed in both the peptides and the proteins. The quenching of Trp fluorescence by acrylamide and iodide is always much greater in the peptides than the proteins, suggesting that the Trp residues are much more accessible to quencher in the peptides than the proteins. Thus, our results suggest that the fluorescence properties of proteins depend to a significant extent on long-range effects that are present in proteins but not in pentapeptides.

This work was supported by National Institutes of Health (GM 37039 GM33216, GM 52483), the Welch Foundation (BE-1060, BE-1281, A1543), and the Tom and Jean McMullin Professorship.

REFERENCES

1. Radivojac, P., L. M. Iakoucheva, C. J. Oldfield, Z. Obradovic, V. N. Uversky, and A. K. Dunker. 2007. Intrinsic disorder and functional proteomics. *Biophys. J.* 92:1439–1456.
2. Sanchez-Puig, N., D. B. Veprintsev, and A. R. Fersht. 2005. Human full-length Securin is a natively unfolded protein. *Protein Sci.* 14: 1410–1418.
3. Pace, C. N., R. W. Alston, and K. L. Shaw. 2000. Charge-charge interactions influence the denatured state ensemble and contribute to protein stability. *Protein Sci.* 9:1395–1398.
4. Strickler, S. S., A. V. Gribenko, T. R. Keiffer, J. Tomlinson, T. Reihle, V. V. Loladze, and G. I. Makhatadze. 2006. Protein stability and surface electrostatics: a charged relationship. *Biochemistry.* 45:2761–2766.
5. Cho, J. H., and D. P. Raleigh. 2005. Mutational analysis demonstrates that specific electrostatic interactions can play a key role in the denatured state ensemble of proteins. *J. Mol. Biol.* 353:174–185.
6. Trefethen, J. M., C. N. Pace, J. M. Scholtz, and D. N. Brems. 2005. Charge-charge interactions in the denatured state influence the folding kinetics of ribonuclease Sa. *Protein Sci.* 14:1934–1938.
7. Cho, J. H., and D. P. Raleigh. 2006. Denatured state effects and the origin of nonclassical ϕ values in protein folding. *J. Am. Chem. Soc.* 128:16492–16493.
8. Arai, M., M. Kataoka, K. Kuwajima, C. R. Matthews, and M. Iwakura. 2003. Effects of the difference in the unfolded-state ensemble on the folding of Escherichia coli dihydrofolate reductase. *J. Mol. Biol.* 329: 779–791.
9. Teale, F. W. 1960. The ultraviolet fluorescence of proteins in neutral solution. *Biochem. J.* 76:381–388.
10. Kronman, M. J., and L. G. Holmes. 1971. The fluorescence of native, denatured and reduced-denatured proteins. *Photochem. Photobiol.* 14: 113–134.
11. Pajot, P. 1976. Fluorescence of proteins in 6-M guanidine hydrochloride. A method for the quantitative determination of tryptophan. *Eur. J. Biochem.* 63:263–269.
12. Garcia, P., M. Desmadril, P. Minard, and J. M. Yon. 1995. Evidence for residual structures in an unfolded form of yeast phosphoglycerate kinase. *Biochemistry.* 34:397–404.
13. Scalley, M. L., S. Nauli, S. T. Gladwin, and D. Baker. 1999. Structural transitions in the protein L denatured state ensemble. *Biochemistry.* 38:15927–15935.
14. Tcherkasskaya, O., V. E. Bychkova, V. N. Uversky, and A. M. Gronenborn. 2000. Multisite fluorescence in proteins with multiple tryptophan residues. APO myoglobin natural variants and site-directed mutants. *J. Biol. Chem.* 275:36285–36294.
15. Chattopadhyay, A., S. S. Rawat, D. A. Kelkar, S. Ray, and A. Chakrabarti. 2003. Organization and dynamics of tryptophan residues

- in erythroid spectrin: novel structural features of denatured spectrin revealed by the wavelength-selective fluorescence approach. *Protein Sci.* 12:2389–2403.
16. Dubey, V. K., and M. V. Jagannadham. 2003. Differences in the unfolding of procerain induced by pH, guanidine hydrochloride, urea, and temperature. *Biochemistry*. 42:12287–12297.
17. Tew, D. J., and S. P. Bottomley. 2001. Probing the equilibrium denaturation of the serpin alpha(1)-antitrypsin with single tryptophan mutants; evidence for structure in the urea unfolded state. *J. Mol. Biol.* 313:1161–1169.
18. Saxena, A. M., J. B. Udagankar, and G. Krishnamoorthy. 2006. Characterization of intra-molecular distances and site-specific dynamics in chemically unfolded Barstar: evidence for denaturant-dependent non-random structure. *J. Mol. Biol.* 359:174–189.
19. Vangala, S., G. Vidugiris, and C. Royer. 1998. Probing the relation between protein structure and intrinsic tryptophan fluorescence using super repressor mutants of the Trp repressor. *J. Fluoresc.* 8:1–11.
20. Nath, U., and J. B. Udagankar. 1997. Folding of tryptophan mutants of Barstar: evidence for an initial hydrophobic collapse on the folding pathway. *Biochemistry*. 36:8602–8610.
21. Nanda, V., S. M. Liang, and L. Brand. 2000. Hydrophobic clustering in acid-denatured IL-2 and fluorescence of a Trp NH-pi H-bond. *Biochem. Biophys. Res. Commun.* 279:770–778.
22. Chattopadhyay, K., E. L. Elson, and C. Frieden. 2005. The kinetics of conformational fluctuations in an unfolded protein measured by fluorescence methods. *Proc. Natl. Acad. Sci. USA*. 102:2385–2389.
23. Merchant, K. A., R. B. Best, J. M. Louis, I. V. Gopich, and W. A. Eaton. 2007. Characterizing the unfolded states of proteins using single-molecule FRET spectroscopy and molecular simulations. *Proc. Natl. Acad. Sci. USA*. 104:1528–1533.
24. Sinha, K. K., and J. B. Udagankar. 2007. Dissecting the non-specific and specific components of the initial folding reaction of Barstar by multi-site FRET measurements. *J. Mol. Biol.* 370:385–405.
25. Shehu, A., L. E. Kaviraki, and C. Clementi. 2007. On the characterization of protein native state ensembles. *Biophys. J.* 92:1503–1511.
26. Tanford, C., K. Kawahara, S. Lapanje, T. M. Hooker, Jr., M. H. Zarlengo, A. Salahuddin, K. C. Aune, and T. Takagi. 1967. Proteins as random coils. 3. Optical rotatory dispersion in 6 M guanidine hydrochloride. *J. Am. Chem. Soc.* 89:5023–5029.
27. Rose, G. D. (editor). 2002. *Advances in Protein Chemistry*, Vol. 62. Elsevier, New York.
28. Matsuo, K., Y. Sakurada, R. Yonehara, M. Kataoka, and K. Gekko. 2007. Secondary-structure analysis of denatured proteins by vacuum-ultraviolet circular dichroism spectroscopy. *Biophys. J.* 92:4088–4096.
29. Tanford, C. 1968. Protein denaturation. *Adv. Protein Chem.* 23:121–282.
30. Miller, W. G., and C. V. Goebel. 1968. Dimensions of protein random coils. *Biochemistry*. 7:3925–3935.
31. Kohn, J. E., I. S. Millett, J. Jacob, B. Zagrovic, T. M. Dillon, N. Cingel, R. S. Dothager, S. Seifert, P. Thiagarajan, T. R. Sosnick, M. Z. Hasan, V. S. Pande, I. Ruczinski, S. Doniach, and K. W. Plaxco. 2004. Random-coil behavior and the dimensions of chemically unfolded proteins. *Proc. Natl. Acad. Sci. USA*. 101:12491–12496.
32. Shortle, D. 2002. The expanded denatured state: an ensemble of conformations trapped in a locally encoded topological space. *Adv. Protein Chem.* 62:1–23.
33. Dill, K. A., and D. Shortle. 1991. Denatured states of proteins. *Annu. Rev. Biochem.* 60:795–825.
34. Denisov, V. P., B. H. Jonsson, and B. Halle. 1999. Hydration of denatured and molten globule proteins. *Nat. Struct. Biol.* 6:253–260.
35. Shortle, D., and M. S. Ackerman. 2001. Persistence of native-like topology in a denatured protein in 8 M urea. *Science*. 293:487–489.
36. Klein-Seetharaman, J., M. Oikawa, S. B. Grimshaw, J. Wirmer, E. Duchardt, T. Ueda, T. Imoto, L. J. Smith, C. M. Dobson, and H. Schwalbe. 2002. Long-range interactions within a nonnative protein. *Science*. 295:1719–1722.
37. Ferreon, A. C., and D. W. Bolen. 2004. Thermodynamics of denaturant-induced unfolding of a protein that exhibits variable two-state denaturation. *Biochemistry*. 43:13357–13369.
38. Mok, Y. K., C. M. Kay, L. E. Kay, and J. Forman-Kay. 1999. NOE data demonstrating a compact unfolded state for an SH3 domain under non-denaturing conditions. *J. Mol. Biol.* 289:619–638.
39. Dyson, H. J., and P. E. Wright. 2002. Insights into the structure and dynamics of unfolded proteins from nuclear magnetic resonance. *Adv. Protein Chem.* 62:311–340.
40. Anil, B., Y. Li, J. H. Cho, and D. P. Raleigh. 2006. The unfolded state of NTL9 is compact in the absence of denaturant. *Biochemistry*. 45:10110–10116.
41. Choy, W. Y., F. A. Mulder, K. A. Crowhurst, D. R. Muhandiram, I. S. Millett, S. Doniach, J. D. Forman-Kay, and L. E. Kay. 2002. Distribution of molecular size within an unfolded state ensemble using small-angle X-ray scattering and pulse field gradient NMR techniques. *J. Mol. Biol.* 316:101–112.
42. Mayor, U., J. G. Grossmann, N. W. Foster, S. M. Freund, and A. R. Fersht. 2003. The denatured state of Engineered Homeodomain under denaturing and native conditions. *J. Mol. Biol.* 333:977–991.
43. Goldenberg, D. P. 2003. Computational simulation of the statistical properties of unfolded proteins. *J. Mol. Biol.* 326:1615–1633.
44. Wong, K. B., J. Clarke, C. J. Bond, J. L. Neira, S. M. Freund, A. R. Fersht, and V. Daggett. 2000. Towards a complete description of the structural and dynamic properties of the denatured state of barnase and the role of residual structure in folding. *J. Mol. Biol.* 296:1257–1282.
45. Fitzkee, N. C., and G. D. Rose. 2005. Sterics and solvation window accessible conformational space for unfolded proteins. *J. Mol. Biol.* 353:873–887.
46. Jha, A. K., A. Colubri, K. F. Freed, and T. R. Sosnick. 2005. Statistical coil model of the unfolded state: resolving the reconciliation problem. *Proc. Natl. Acad. Sci. USA*. 102:13099–13104.
47. Tran, H. T., and R. V. Pappu. 2006. Toward an accurate theoretical framework for describing ensembles for proteins under strongly denaturing conditions. *Biophys. J.* 91:1868–1886.
48. Thurlkill, R. L., G. R. Grimsley, J. M. Scholtz, and C. N. Pace. 2006. Hydrogen bonding markedly reduces the pK of buried carboxyl groups in proteins. *J. Mol. Biol.* 362:594–604.
49. Trevino, S. R., K. Gokulan, S. Newsom, R. L. Thurlkill, K. L. Shaw, V. A. Mitkevich, A. A. Makarov, J. C. Sacchettini, J. M. Scholtz, and C. N. Pace. 2005. Asp79 makes a large, unfavorable contribution to the stability of RNase Sa. *J. Mol. Biol.* 354:967–978.
50. Trevino, S. R., J. M. Scholtz, and C. N. Pace. 2007. Amino acid contribution to protein solubility: Asp, Glu, and Ser contribute more favorably than the other hydrophilic amino acids in RNase Sa. *J. Mol. Biol.* 366:449–460.
51. Sevcik, J., V. S. Lamzin, Z. Dauter, and K. S. Wilson. 2002. Atomic resolution data reveal flexibility in the structure of RNase Sa. *Acta Crystallogr. D Biol. Crystallogr.* 58:1307–1313.
52. Laurents, D., J. M. Perez-Canadillas, J. Santoro, M. Rico, D. Schell, C. N. Pace, and M. Bruix. 2001. Solution structure and dynamics of ribonuclease Sa. *Proteins*. 44:200–211.
53. Laurents, D. V., B. M. Huyghues-Despointes, M. Bruix, R. L. Thurlkill, D. Schell, S. Newsom, G. R. Grimsley, K. L. Shaw, S. Trevino, M. Rico, J. M. Briggs, J. M. Antosiewicz, J. M. Scholtz, and C. N. Pace. 2003. Charge-charge interactions are key determinants of the pK values of ionizable groups in ribonuclease Sa (pI = 3.5) and a basic variant (pI = 10.2). *J. Mol. Biol.* 325:1077–1092.
54. Huyghues-Despointes, B. M., R. L. Thurlkill, M. D. Daily, D. Schell, J. M. Briggs, J. M. Antosiewicz, C. N. Pace, and J. M. Scholtz. 2003. pK values of histidine residues in ribonuclease Sa: effect of salt and net charge. *J. Mol. Biol.* 325:1093–1105.
55. Alston, R. W., L. Urbanikova, J. Sevcik, M. Lasagna, G. D. Reinhart, J. M. Scholtz, and C. N. Pace. 2004. Contribution of single tryptophan residues to the fluorescence and stability of ribonuclease Sa. *Biophys. J.* 87:4036–4047.

56. Pace, C. N., and J. M. Scholtz. 1997. Measuring the conformational stability of a protein. In *Protein Structure: A Practical Approach*. T. E. Creighton, editor. IRL Press, Oxford. 299–321.
57. Hebert, E. J., G. R. Grimsley, R. W. Hartley, G. Horn, D. Schell, S. Garcia, V. Both, J. Sevcik, and C. N. Pace. 1997. Purification of ribonucleases Sa, Sa2, and Sa3 after expression in *Escherichia coli*. *Protein Expr. Purif.* 11:162–168.
58. Hebert, E. J., A. Giletto, J. Sevcik, L. Urbanikova, K. S. Wilson, Z. Dauter, and C. N. Pace. 1998. Contribution of a conserved asparagine to the conformational stability of ribonucleases Sa, Ba, and T1. *Biochemistry*. 37:16192–16200.
59. Pace, C. N., F. Vajdos, L. Fee, G. Grimsley, and T. Gray. 1995. How to measure and predict the molar absorption coefficient of a protein. *Protein Sci.* 4:2411–2423.
60. Alston, R. W., M. Lasagna, J. M. Scholtz, G. D. Reinhart, and C. N. Pace. 2008. Peptide sequence and conformation strongly influence tryptophan fluorescence. *Biophys. J.* 94:2280–2287.
61. Pace, C. N., E. J. Hebert, K. L. Shaw, D. Schell, V. Both, D. Krajcikova, J. Sevcik, K. S. Wilson, Z. Dauter, R. W. Hartley, and G. R. Grimsley. 1998. Conformational stability and thermodynamics of folding of ribonucleases Sa, Sa2 and Sa3. *J. Mol. Biol.* 279:271–286.
62. Eftink, M. R. 1991. Fluorescence Techniques for Studying Protein-Structure. *Methods Biochem. Anal.* 35:127–205.
63. Vivian, J. T., and P. R. Callis. 2001. Mechanisms of tryptophan fluorescence shifts in proteins. *Biophys. J.* 80:2093–2109.
64. Callis, P. R. 1997. 1La and 1Lb transitions of tryptophan: applications of theory and experimental observations to fluorescence of proteins. *Methods Enzymol.* 278:113–150.
65. Chakraborty, S., V. Ittah, P. Bai, L. Luo, E. Haas, and Z. Peng. 2001. Structure and dynamics of the alpha-lactalbumin molten globule: fluorescence studies using proteins containing a single tryptophan residue. *Biochemistry*. 40:7228–7238.
66. Cowgill, R. W. 1967. Fluorescence and protein structure. X. Reappraisal of solvent and structural effects. *Biochim. Biophys. Acta.* 133:6–18.
67. Eftink, M. R., Y. Jia, D. Hu, and C. A. Ghiron. 1995. Fluorescence studies with tryptophan analogues: excited state interactions involving the side chain amino group. *J. Phys. Chem.* 99:5713–5723.
68. Hellings, M., M. De Maeyer, S. Verheyden, Q. Hao, E. J. Van Damme, W. J. Peumans, and Y. Engelborghs. 2003. The dead-end elimination method, tryptophan rotamers, and fluorescence lifetimes. *Biophys. J.* 85:1894–1902.
69. Pan, C. P., and M. D. Barkley. 2004. Conformational effects on tryptophan fluorescence in cyclic hexapeptides. *Biophys. J.* 86:3828–3835.
70. Callis, P. R., and T. Q. Liu. 2004. Quantitative prediction of fluorescence quantum yields for tryptophan in proteins. *J. Phys. Chem. B.* 108:4248–4259.
71. Chen, J., S. L. Flaugh, P. R. Callis, and J. King. 2006. Mechanism of the highly efficient quenching of tryptophan fluorescence in human gammaD-crystallin. *Biochemistry*. 45:11552–11563.
72. Bowler, B. E. 2007. Thermodynamics of protein denatured states. *Mol. Biosyst.* 3:88–99.
73. Baldwin, R. L. 2002. Making a network of hydrophobic clusters. *Science*. 295:1657–1658.
74. Eftink, M. R., and K. A. Hagaman. 1986. Viscosity dependence of the solute quenching of the tryptophanyl fluorescence of proteins. *Biophys. Chem.* 25:277–282.